Schizophrenia Bulletin Advance Access published July 10, 2015

Schizophrenia Bulletin
doi:10.1093/schbul/sbv092

EEG-Informed fMRI Reveals a Disturbed Gamma-Band–Specific Network in Subjects at High Risk for Psychosis

Gregor Leicht*[,1,3], Sebastian Vauth[1,3], Nenad Polomac[1], Christina Andreou[1], Jonas Rauh[1], Marius Mußmann[1], Anne Karow[2], and Christoph Mulert[1]

[1]Department of Psychiatry and Psychotherapy, Psychiatry Neuroimaging Branch (PNB) and [2]Department of Psychiatry and Psychotherapy, University Medical Center Hamburg-Eppendorf, Hamburg, Germany

[3]These authors contributed equally to the article.

*To whom correspondence should be addressed; University Medical Center Hamburg-Eppendorf, Department of Psychiatry and Psychotherapy, Psychiatry Neuroimaging Branch (PNB), Martinistrasse 52, D-20246 Hamburg, Germany; tel: +49-40-7410-59519, fax: +49-40-7410-59805, e-mail: g.leicht@uke.de

Objectives. **Abnormalities of oscillatory gamma activity are supposed to reflect a core pathophysiological mechanism underlying cognitive disturbances in schizophrenia. The auditory evoked gamma-band response (aeGBR) is known to be reduced across all stages of the disease. The present study aimed to elucidate alterations of an aeGBR-specific network mediated by gamma oscillations in the high-risk state of psychosis (HRP) by means of functional magnetic resonance imaging (fMRI) informed by electroencephalography (EEG).** ***Methods.*** **EEG and fMRI were simultaneously recorded from 27 HRP individuals and 26 healthy controls (HC) during performance of a cognitively demanding auditory reaction task. We used single trial coupling of the aeGBR with the corresponding blood oxygen level depending response (EEG-informed fMRI).** ***Results.*** **A gamma-band–specific network was significantly lower active in HRP subjects compared with HC (random effects analysis, $P < .01$, Bonferroni-corrected for multiple comparisons) accompanied by a worse task performance. This network involved the bilateral auditory cortices, the thalamus and frontal brain regions including the anterior cingulate cortex, as well as the bilateral dorsolateral prefrontal cortex.** ***Conclusions.*** **For the first time we report a reduced activation of an aeGBR-specific network in HRP subjects brought forward by EEG-informed fMRI. Because the HRP reflects the clinical risk for conversion to psychotic disorders including schizophrenia and the aeGBR has repeatedly been shown to be altered in patients with schizophrenia the results of our study point towards a potential applicability of aeGBR disturbances as a marker for the prediction of transition of HRP subjects to schizophrenia.**

Key words: prodromal state of schizophrenia/auditory evoked gamma-band response/simultaneous EEG-fMRI/anterior cingulate cortex/auditory cortex

Introduction

The mediation of cognitive and perceptual processes by terms of synchronization of neuronal oscillations in the gamma-band frequency range (above 40 Hz) is supposed to be a fundamental process in brain function and communication.[1–5] Thus, abnormalities of the synchronization of gamma oscillations are thought to cause disturbances with respect to the coordination of processes involving multiple brain areas.[6] Schizophrenia is hypothesized to result from a disrupted structural and functional connectivity within the brain.[7–9] Hence, abnormalities of oscillatory gamma activity may reflect a core pathophysiological mechanism underlying cognitive disturbances and other symptoms of schizophrenia.[10] This is further supported by evidence of the crucial role of a microcircuit involving parvalbumin-positive GABAergic interneurons and glutamatergic pyramidal cells for the generation of gamma oscillations,[11,12] which is disrupted in patients with schizophrenia and in pharmacological or genetic models of the illness.[13–15] Accordingly, several studies using electroencephalography (EEG) and magnetoencephalography (MEG) reported alterations of gamma-band oscillations in schizophrenia both with regard to deficits in sensory processing[16–25] and cognitive functions.[25–31]

The early auditory evoked gamma-band response (aeGBR, 25–100 msec upon the presentation of an auditory stimulus[32]) has been shown to be influenced by attentional processes[33–35] and task difficulty.[36,37] It is reduced across all stages of schizophrenia: first-episode,[38,39] chronic patients,[29,40] and symptom-free first-degree relatives of patients.[41,42] Therefore and in reference to the association with the biologically plausible mechanism of a disrupted microcircuit involving interneurons and pyramidal cells, the reduced aeGBR has been suggested as a

putative endophenotype[43] for schizophrenia.[41,44] Recently, Perez and colleagues[45] reported that an aeGBR power reduction is already present during the prodromal phase of the disease in individuals at clinical high risk for psychosis (HRP). Accordingly, alterations of the aeGBR might represent a promising biomarker for the identification of HRP subjects with an increased risk of conversion to schizophrenia.

Besides the origin of the aeGBR in the primary auditory cortex[32] both EEG-based source localization[37,40] and single trial coupling of EEG and functional magnetic resonance imaging (fMRI)[46] revealed an additional aeGBR generator in the medial prefrontal cortex and the dorsal anterior cingulate cortex (dACC) during a cognitively demanding auditory choice reaction task. Patients with schizophrenia exhibited a reduced activity in the auditory cortex and the dACC/medial frontal gyrus region underlying the reduced gamma activity measured on the scalp.[40] The present study aimed to elucidate alterations of this network mediated by gamma oscillations in the high-risk state of schizophrenia by means of EEG-informed fMRI in order to further characterize a candidate biomarker for the prediction of transition to psychosis. We hypothesized that the activation of a gamma-mediated frontotemporal network during the performance of a cognitively demanding auditory reaction task would be reduced in individuals at HRP.

Methods and Materials

Ethics Statement

The present study was part of a larger project investigating resting-state and task-related brain connectivity in schizophrenia by means of EEG, MEG, and simultaneous EEG-fMRI, within the context of the Collaborative Research Centre 936 ("multi-site communication in the brain," www.sfb936.net). The study was approved by the Ethics Committee of the Medical Association Hamburg and carried out in accordance with the seventh revision of the Declaration of Helsinki (2013). Written informed consent was obtained from all participants after the aim of the study and the nature of the procedures had been fully explained.

Participants

27 HRP individuals and 26 healthy controls (HC) were included in the study. For details on the recruitment please see the supplementary material. Exclusion criteria for all participants were current substance abuse or dependence, and presence of major somatic or neurological disorders. For HC, additional exclusion criteria were any previous psychiatric disorder or treatment, and a family history of psychotic disorders. The presence of inclusion/exclusion criteria was assessed by means of a semi-structured interview conducted by a clinical psychiatrist or psychiatric trainee with at least 4 years of clinical experience. Three HRP individuals (error rates bigger than 33% of the target trials) and 2 HC (anatomical abnormality and poor EEG data quality respectively) were excluded from further analysis resulting in 24 participants per group.

The high-risk state was defined according to criteria of the Early Detection and Intervention program of the German Research Network on Schizophrenia (GNRS;[47]) detailed in the supplementary material. According to the GNRS criteria previous studies have differentiated between an early (E-HRP) and a late HRP (L-HRP).[48] In the present study, the majority of HRP participants met criteria for the L-HRP ($n = 17$).

The Mini International Neuropsychiatric Interview[49] was used in HRP individuals in order to rule out a diagnosis of schizophrenia spectrum disorder and to document comorbid psychiatric diagnoses (mood disorder $n = 11$; anxiety/obsessive-compulsive disorder $n = 6$; substance related disorders $n = 6$ [all subjects currently abstinent]; and personality disorders $n = 1$; for more details please see supplementary material). HRP subjects were additionally assessed with the Scale of Prodromal Symptoms (SOPS[50]; rater training detailed in supplementary material), whereby 3 subscores for negative/disorganization, depressive/stress and positive symptoms were created according to a recent factor analysis of the scale[51] (data not available for 3 HRP subjects).

The groups were matched with respect to age, sex, and educational level. All subjects had hearing better than 30 db at a pitch of 1000 Hz. Five out of 24 HRP individuals were receiving 1 or 2 atypical antipsychotics at the time of participation in the study (aripiprazole [$n = 2$; mean dosage per day: 3.75 mg], olanzapine [$n = 2$; 3.75 mg], and quetiapine [$n = 3$; 175 mg]). Moreover, 4 HRP subjects were currently in treatment with antidepressants. No subjects were receiving mood stabilizers, benzodiazepines, or anticholinergic agents. Demographic characteristics of the groups, and clinical characteristics of HRP participants, are presented on table 1.

Paradigm

We used an auditory reaction task[52] that had been earlier shown to increase the aeGBR amplitude[37] and the aeGBR-specific blood-oxygen-level dependent (BOLD) response within the ACC and the auditory cortex.[46] During the experiment 300 tones of 3 different pitches (33% 700 Hz, 33% 1000 Hz, and 33% 1300 Hz; duration: 200 ms, generated using the Presentation software version 17 installed on a personal computer which was placed outside the shielded MR room) were presented with pseudo-randomized interstimulus intervals (ISI: 2.5–7.5 s; mean 3.8 s) via MRI-compatible electrostatic headphones (MR confon). Tones at a pitch of 700 Hz and 1300 Hz had to be responded to as fast and accurately as possible per button-press with the left or the right index finger, respectively (target stimuli). Reaction times and

Table 1. Clinical and Demographic Characteristics of the 2 Participant Groups

	Healthy Controls		High-Risk Subjects			
	N		*N*		T/χ^2	*P*
Gender (m/f)	11/13		13/11		0.33	0.56
	Mean	(*SD*)	Mean	(*SD*)		
Age	23.0	3.7	21.5	3.6	1.47	0.15
SOPS scores						
Negative/disorganization			6.5	6.2		
Depressive/stress			4.1	3.2		
Positive			5.1	3.8		

Note: SOPS, Scale of Prodromal Symptoms.

error rates (number of incorrect responses or missing responses within 2000 ms after target stimulus presentation divided by the number of presented target stimuli) were registered during the experimental run.

fMRI Parameters and Analysis

Imaging was performed on a 3-T MR scanner (Siemens Magnetom Trio) equipped with a 12 channel head coil using a standard gradient echo-planar imaging T2*-sensitive sequence for functional BOLD imaging. Twenty-four slices covering the whole brain (456 volumes; TR = 2.5 s; TA = 1.4 s; TE = 30 ms; FOV = 216/216 mm; matrix = 72 × 72; interleaved slice acquisition; slice thickness = 4 mm; interslice gap = 1 mm; resulting pixel size = 3 × 3 mm) were acquired in the same position as a 3-dimensional MPRAGE data set (T1-weighted). We used this "sparse sampling design" with EEG acquisition interleaved with MR image acquisition[46,53–55] and MR-acquisition-free periods of 1.1 s in order to avoid disturbances of gradient artifacts concerning our EEG signal of interest and disturbances of our auditory stimuli with the scanner noise. During the acquisition of fMRI data the vacuum pump of the MRI scanner was switched off in order to avoid EEG artifacts within the gamma-band frequency range.

The postprocessing of fMRI data was conducted using the BrainVoyager QX software package (version 2.8, Rainer Goebel). Motion correction (trilinear/sinc interpolation) and data smoothing (temporal high-pass GLM-Fourier filter) including linear trend removal was applied before alignment of the functional data with the 3-dimensional anatomical volumes, transformation into the Talairach space, and interpolation to a resolution of 3 × 3 × 3 mm. For the statistical analysis, regression coefficients were estimated based on a general linear model (GLM). The multiple regression analysis was performed on the 3-dimensional functional volume time courses (1 for each subject). The design matrix for the fMRI analysis (without adding EEG information) contained modeled BOLD response functions corresponding to each of the 3 stimulus events convolved with a canonical hemodynamic response function (2 Gamma HRF) which resulted in 3 different regressors. The mean contrast images of target tones vs baseline are presented at a significance level of $P < .001$ (random effects analysis, corrected for multiple comparisons across the whole brain using Bonferroni correction).

EEG Acquisition

EEG recordings took place within the MRI scanner during acquisition of fMRI data. Subjects were lying on their back and were asked to keep the eyes open and look at a fixation cross projected to a mirror mounted on the head coil. We used 2 EEG amplifiers specifically developed for operation in the MRI scanner environment and particularly avoiding saturation by magnetic activity (BrainAmp MRplus; Brain Products). The EEG recording was performed in alternating current mode with 62 active EEG electrodes (sintered silver and silver-chlorid) mounted on an elastic cap (BrainCapMR 64, Brain Products) using the BrainVision Recorder software (Version 1.10, Brain Products). Electrodes were arranged according to a modified 10/10 system (reference electrode: FCz; ground: AFz). The electrode skin impedance was kept below 10 kΩ. Data were collected with a sampling rate of 5000 Hz and an analogous band-pass filter (0.1–250 Hz). The amplitude resolution was set to 0.1 μV in order to be able to measure low amplitude gamma oscillations.

EEG Preprocessing

The EEG data analysis was carried out using Brain Vision Analyzer (BVA) Version 2.0 (Brain Products). Offline, the continuous EEG data were segmented into gradient artifact free epochs (MR-acquisition-free periods of 1.1 s), filtered using a band-pass (30–100 Hz, Butterworth Zero Phase Filter, slope 48 db/oct) and a notch filter (50 Hz),

resampled to a sampling rate of 1000 Hz and re-referenced to common average reference. Due to our "sparse sampling approach" the EEG timeframe of interest including the aeGBR to the target stimuli was not affected by gradient artifacts. Ballistocardiogram (BCG) artifacts have a frequency spectrum at around 3–15 Hz,[56] therefore not affecting the frequency range of interest for the present study. This issue has explicitly been investigated in our previous study on the aeGBR-specific BOLD response.[46] Hence, no gradient artifact or BCG artifact correction was performed.

Next, we identified the subjects' individual peak frequencies of the aeGBR (method described in supplementary material). This information was used in an independent component analysis (ICA) based approach in order to identify the aeGBR power information on single trial level. ICA (Algorithm: Infomax [Gradient] extended biased, calculating components corresponding to an eigenvalue >0.05) was performed on appended single trial epochs with a length of 500 ms starting 250 ms prior to the target stimuli (number of calculated components: HRP 61.3 [*SD*: 0.9], HC 61.3 [*SD*: 1.3]; no significant difference). After baseline correction (baseline: 250 ms prior to the stimulus) and averaging of the resulting components over trials for every subject a continuous wavelet transformation with a complex Morlet wavelet (real values [μV^2], 10 frequency layers distributed on a logarithmic scale, Morlet parameter $c = 5$, Gabor Normalization) for the frequency range from 30 to 50 Hz was performed. Components including the aeGBR information were identified by showing a 3 times higher gamma power peak value within the timeframe 30–120 ms after stimulus presentation compared with the gamma power peak value within a baseline of 100 ms before stimulus presentation in the subjects' individual peak frequency layer. Only the components carrying the aeGBR information were back-projected to the sensor space (number of aeGBR carrying components: HRP 11.4 [*SD*: 5.9], HC 10.2 [*SD*: 4.4]; no significant difference). On sensor single trial level, a baseline correction (baseline: 100 ms prior to the stimulus) was performed followed by a transformation with a complex Morlet wavelet (parameters see above) for the frequency range from 30 to 50 Hz. The single trial aeGBR power peak amplitudes were defined as the highest value of the identified peak frequency layer within the timeframe 30–100 ms after stimulus presentation at the electrode Cz. In order to be able to compare the aeGBR to targets with the aeGBR to nontargets the analysis outlined above was repeated for nontargets starting with the ICA on appended single trial nontarget epochs. The aeGBR single trial time series including 1 aeGBR power value for every target stimulus were forwarded to the EEG-informed fMRI analysis. AeGBR values exceeding the mean amplitude value of a single trial time series by more than 1.4 standard deviations were considered as artifacts and set to the individual mean value.

In order to investigate group differences with respect to the aeGBR the wavelet transformation was also applied to averaged target and nontarget trials, respectively. Using these averages the aeGBR power peaks were parametrized as the highest value of the peak frequency layer within the timeframe 30–100 ms after stimulus presentation at the electrode Cz. Methods with respect to the calculation of the aeGBR phase locking factor (PLF) are detailed in the supplementary material.

EEG-Informed fMRI Analysis

The aeGBR time series information was used to calculate regressors for the EEG-informed fMRI GLM analysis. For that purpose, every target stimulus presentation (constant amplitude) of the target stimulus function X_G was replaced by the aeGBR power value corresponding to the respective target stimulus. This resulted in the function X_{aeGBR} representing the aeGBR power variation over trials. X_G represented BOLD activation not related to the aeGBR. In order to find fMRI results that are specifically related to the aeGBR power measure and not to some general feature of the target detection process we used Schmidt-Gram orthogonalization as suggested previously[57] and applied by our group in several studies.[46,55,58–60] In the present study, X_{aeGBR} was orthogonalized with respect to X_G removing that part of X_{aeGBR} which was correlated to X_G (for a detailed description please see[46,55]).

The design matrix for the EEG-informed fMRI analysis (GLM, performed on the 3-dimensional functional volume time courses, see above) contained 3-modeled BOLD response functions corresponding to X_G, X'_{aeGBR}, and the nontarget stimulus function each of them convolved with a canonical hemodynamic response function (2 Gamma HRF). An event-related analysis was then performed for each subject revealing the contrast between aeGBR-specific BOLD response and baseline volumes (first level analysis). The resulting contrast images were entered into a second level group analysis treating intersubject variability as a random effect. Results are presented at a significance level of $P < .01$ (corrected for multiple comparisons across the whole brain using Bonferroni correction). Labeling of anatomical regions was based on the Talairach Daemon (http://www.talairach.org/daemon.html).

Five regions of interest (ROI) were selected in regions showing significantly lower aeGBR-specific activity in HRP subjects compared with HC and based on previous knowledge on the localization of aeGBR generators[37,40,46,61]: left and right auditory cortex, dACC and left and right dorsolateral prefrontal cortex (DLPFC; methods detailed in supplementary material).

Statistical Analyses

All statistical analyses were performed using the SPSS software package (21.0). For the comparison of the 2 groups on educational level and gender differences, the

chi-square test was used. In order to check for significant group differences with respect to reaction times, error rates and age 2-sided *t* tests for independent samples were used. AeGBR power amplitude and PLF differences were tested for group differences using a 1-sided *t* test following the hypothesis of an aeGBR power and PLF reduction in schizophrenia which is based on several previous reports.[39–42,45] Correlational analyses were conducted using Spearman's rho. Further statistical subanalyses are detailed in the supplementary material.

Results

HRP subjects (693 ms, *SD* 125) showed significantly longer reaction times compared with HC (625 ms, *SD* 97; $T[df = 46] = 2.1$, $P = .04$). This was also true for the 17 L-HRP subjects (716 ms, *SD* 133) compared with HC ($T[df = 39] = 2.5$, $P = .02$). Moreover, we found higher error rates in HRP subjects (8.0 %) compared with HC (6.5 %), although this difference failed to get significant. Reaction times (rho = 0.449, $P = .04$) and error rates (rho = 0.586, $P = .005$) showed a significant positive correlation with the severity of negative symptoms in the HRP group (not with other SOPS subscores).

Both the analysis conducted to indentify the subjects' individual peak frequencies of the aeGBR (see supplementary figure 1) and our ICA based approach for the identification of the aeGBR power information on the single trial level (see figure 1) revealed an increase of evoked gamma activity (electrode Cz) around a frequency of 40 Hz and about 50 ms after target stimulus presentation in both groups. Moreover, in both analyses the HRP group showed a smaller aeGBR to target stimuli compared with HC (see figure 1 and supplementary figure 1) and the detection of aeGBR power peaks revealed significant lower values in HRP subjects (0.012 μV^2, *SD*: 0.024) compared with the HC (0.043 μV^2, *SD*: 0.085; $T[df = 46] = 1.72$, $P = .047$). The subgroup of L-HRP subjects also showed diminished aeGBR power amplitudes (0.015 μV^2, *SD*: 0.028) compared with HC. However, this difference was not significant, probably due to the smaller sample size. The HRP group showed a statistical trend towards reduced PLF values (HRP: 0.25 [*SD* 0.13]; HC: 0.31 [*SD* 0.17]; $T[df = 46] = 1.35$, $P = .092$). There was no significant difference between groups with respect to the latency of the target aeGBR peaks at Cz (mean latencies: HRP: 55.9 ms [*SD*: 22.7], HC: 55.9 ms [*SD*: 21.4]) or with respect to the aeGBR to nontargets (HRP: 0.022 μV^2 [*SD*: 0.041], HC:

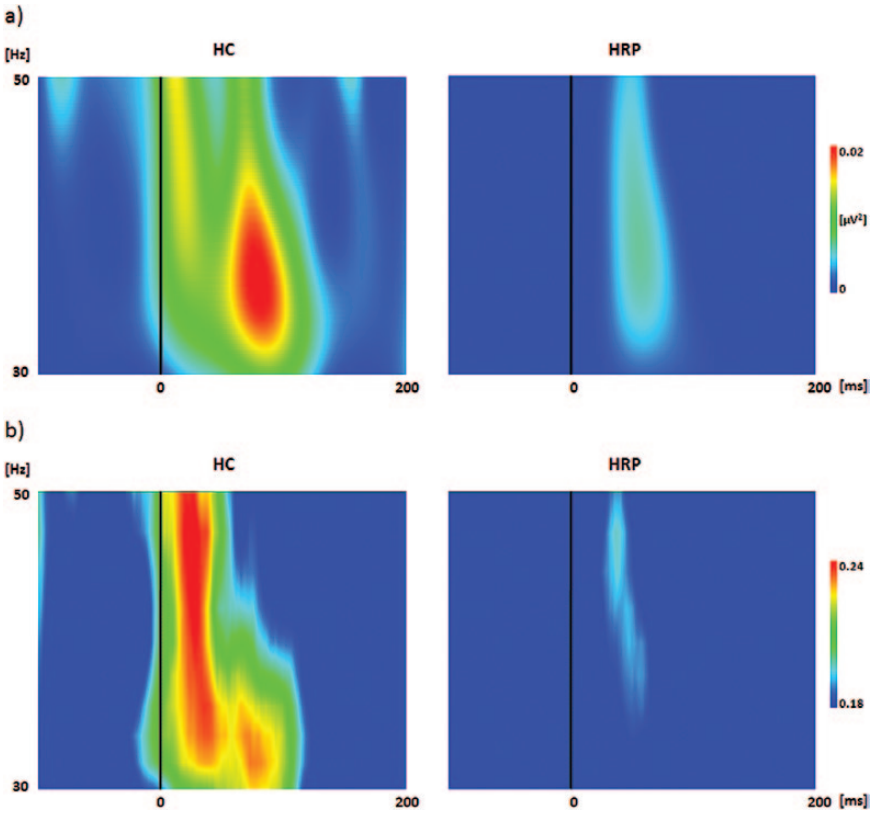

Fig. 1. Auditory evoked gamma-band response (aeGBR) power (a) and phase locking factor (b): group averages for healthy controls (HC) and subjects at clinical high risk for psychosis (HRP) for epochs from 100 ms prior to target stimulus presentation to 200 ms poststimulus and a frequency range from 30 to 50 Hz. An increase of aeGBR power and phase locking can be observed at about 50 ms after stimulus presentation (black line). For the purpose of visualization of the aeGBR results the wavelet transformation was recalculated using 100 frequency layers.

0.030 [*SD*: 0.100]). The statistical comparison of target and nontarget trials revealed no significant effect of the factor target vs nontarget ($F = 0.01$, $P = .91$) and no significant interaction of this factor with group membership ($F = 1.0$, $P = .32$). Neither reaction time nor error rate was significantly associated with aeGBR responses for the whole participant group as well as for each of the participant groups separately. This was also true for a trial specific analysis on the within subject level. Moreover, there was no significant correlation between aeGBR power and the severity of symptoms (3 SOPS subscores) in the HRP group.

The conventional fMRI analysis for the HC group revealed activations of the bilateral auditory cortices, the medial frontal lobe including supplementary motor cortex and ACC, the DLPFC, the thalamus and other regions such as sensorimotor cortex, occipital cortex, precuneus, insula and cerebellum (see figure 2a). Using the same level of significance HRP subjects showed similar locations of activity except the activations within the DLPFC, the precuneus and the occipital cortex (see figure 2b). However, after Bonferroni correction for multiple comparisons we found no significant group differences.

In contrast, the EEG-informed fMRI analysis (aeGBR-specific BOLD signal) revealed a significantly lower activity of a network mediated by gamma oscillations in HRP subjects compared with HC (random effects analysis, $P < .01$, Bonferroni-corrected, see figure 3). Amongst others, this network involved the bilateral auditory cortices, the thalamus and frontal brain regions including the ACC as well as the bilateral DLPFC (see table 2). Within-group results of the EEG-informed fMRI analysis are presented in the supplementary material. Repeating the analysis for comparison of both the subgroup of L-HRP subjects as well as a subgroup of HRP individuals without substance related disorders ($n = 18$) with HC revealed similar results at a lower level of significance. There was no significant correlation between aeGBR-specific activations of the ROIs and the severity of symptoms (3 SOPS subscores) in the HRP group.

Discussion

The present study used an auditory reaction task in order to investigate alterations of the aeGBR-specific BOLD response to task relevant auditory stimulation in HRP individuals by means of EEG-informed fMRI. For the first time we report a reduced activation of a gamma-band specific network involving thalamus, auditory cortices, and frontal regions such as the ACC and the DLPFC in the high-risk state of psychosis brought forward by means of simultaneously recorded EEG and fMRI. HRP subjects showed a significantly diminished aeGBR compared with HC and significantly increased reaction times. Interestingly, the conventional fMRI analysis did not reveal significant differences between groups after Bonferroni correction for multiple comparisons. In contrast, the single trial coupling of aeGBR power peaks and the corresponding BOLD response revealed very robust group differences using Bonferroni correction and treating the inter-subject variability as a random effect.

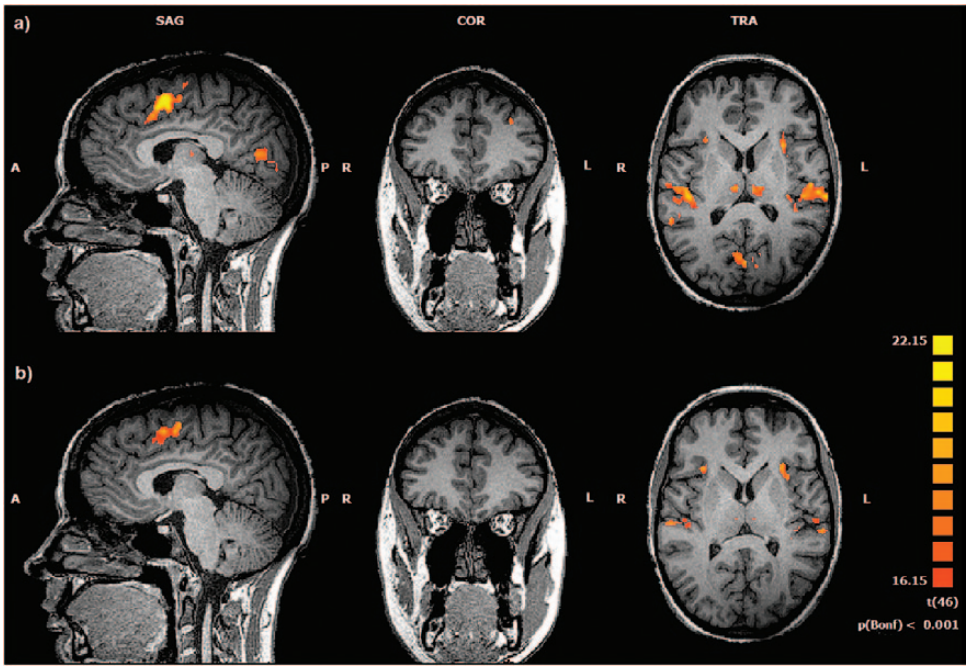

Fig. 2. Conventional fMRI analysis: BOLD response to target stimuli. (a) healthy controls (Talairach coordinates $x = 5$, $y = 36$, $z = 13$). (b) subjects at clinical high risk for psychosis (Talairach coordinates $x = 5$, $y = 36$, $z = 10$). Random effects analysis, $P < .001$ (Bonferroni corrected for multiple comparisons). SAG: sagittal; COR: coronary; TRA: transversal; A: anterior; P: posterior; R: right; L: left.

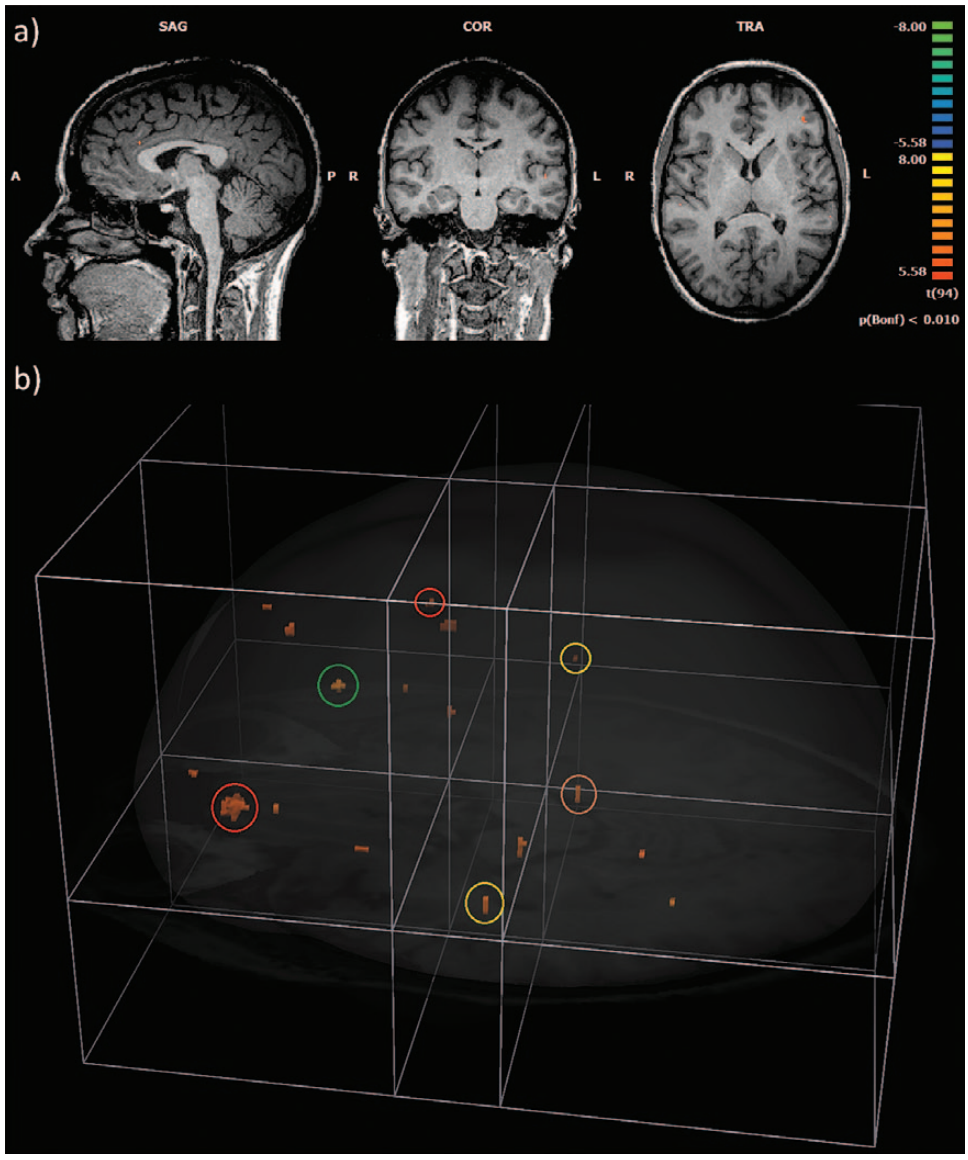

Fig. 3. EEG-informed fMRI analysis: aeGBR-specific BOLD response to target stimuli revealed by single-trial coupling of aeGBR power variation and corresponding BOLD response. Second level group contrast revealing brain regions with significantly higher aeGBR-specific fMRI activations in HC compared with HRP individuals. Random effects analysis, $P < .01$, Bonferroni corrected for multiple comparisons. Results are displayed in slices at Talairach coordinates $x = -3$, $y = -16$ and $z = 10$ (a) as well as in a glass brain view (b). In the latter, significant group differences are visible within the left and right DLPFC (red circles), the ACC (green), the left and right auditory cortex (yellow) and the thalamus (brown). SAG: sagittal; COR: coronary; TRA: transversal; A: anterior; P: posterior; R: right; L: left.

Our results are in line with several studies reporting a relationship between cognitive functions (such as attention) and evoked gamma-band oscillations.[31,35,62] The HRP subjects investigated in our study are characterized by an increased risk of up to 30% for developing a psychotic disorder within 3 years.[63] Though, the extent of the fraction of our HRP subjects converting to schizophrenia is unknown. However, because the high-risk state for psychosis reflects the clinical risk for conversion to psychotic disorders including schizophrenia, the findings of our study correspond to a large body of publications reporting alterations of gamma-band oscillations in schizophrenia (for review see[14]).Especially, the aeGBR, which is also known to be affected by cognitive processes,[34,36,37] has been shown to be disturbed in schizophrenia.[40] Correspondent findings across all stages of the disease (see introduction) including symptom-free first-degree-relatives[41,42] and subjects at high risk for psychosis[45] and a study of Hall and colleagues[44] demonstrating that both aeGBR power and phase locking are heritable traits suggest this biomarker as a putative endophenotype of the disease according to the criteria for the identification of an endophenotype defined by.[64] This is further supported by the fact that the reduction of the

Table 2. EEG-Informed fMRI Analysis: Brain Regions With Significantly Higher aeGBR-Specific fMRI Activations in HC Compared With HRP Individuals (Second Level Group Contrast, $P < .01$, Bonferroni Corrected for Multiple Comparisons)

Region	Talairach Coordinates			Max *t* Value
	x	*y*	*z*	
L anterior cingulate cortex	−4	25	24	7.39
L middle frontal gyrus	−41	40	11	7.15
L cerebellum	−22	−29	−25	7.07
L lentiform nucleus	−22	−20	−4	6.90
R inferior frontal gyrus	47	8	18	6.44
L fusiform gyrus	−40	−50	−15	6.20
L inferior temporal gyrus	−47	−56	0	6.14
L cerebellum	−30	−44	−23	6.08
R precentral gyrus	32	10	30	6.03
L superior temporal gyrus	−52	−17	−2	6.02
R superior temporal gyrus	38	4	−15	6.01
R claustrum	29	16	9	5.94
L superior frontal gyrus	−10	40	45	5.84
R superior temporal gyrus	53	−23	9	5.72
Brainstem (pons)	−1	−20	−34	5.66
L cingulate gyrus	−13	−2	39	5.65
L middle frontal gyrus	−40	49	18	5.63
L cingulate gyrus	−1	31	27	5.62
L medial frontal gyrus	−10	34	40	5.60

Note: EEG, electroencephalography; fMRI, functional magnetic resonance imaging; HC, healthy controls; HRP, high-risk for psychosis; L, left; R, right.

aeGBR in schizophrenia matches the pathophysiological hypothesis of a disturbed neural microcircuit involving cortical glutamatergic pyramidal cells and inhibitory GABAergic parvalbumin-positive interneurons (PPI) in schizophrenia,[15,65] which is also known to be critically involved in the generation of gamma oscillations.[12] In line with this, there are different reports on alterations of the GABAergic inhibitory system in schizophrenic patients which are mainly restricted to fast-spiking PPIs.[66,67] In this context our result of a diminished aeGBR-specific BOLD response in the ACC matches the finding of postmortem studies pointing to PPI abnormalities in the ACC in patients with schizophrenia[68,69] and a report on a correlation between a significantly reduced GBR to a conditioned tone with a decreased density of PPIs in the medial prefrontal cortex in an animal model of schizophrenia.[70] Our finding of a reduced aeGBR-specific activation of the DLPFC is consistent with deficits of the GABAergic and glutamatergic neurotransmission in the DLPFC in schizophrenia.[71,72]

Compared with conventional fMRI analyses EEG-informed fMRI adds the important information of the specific neuronal oscillatory mode involved in the functional relationships between brain regions.[73] Notably, correlations between oscillatory EEG phenomena and BOLD signal are especially high in the gamma-band frequency range.[74–78] Thus, with respect to the present study, aeGBR-informed fMRI could be closer related to the crucial pathophysiological mechanism separating HRP subjects and HC. This might be reflected by our observation of a superior separation between groups using EEG-informed fMRI compared with the conventional fMRI analysis.

The results of our aeGBR-specific fMRI analysis are in line with previous findings in healthy subjects using a similar study design[46] and with the EEG-based localization of aeGBR generators in the bilateral auditory cortices and the medial prefrontal cortex including the dorsal ACC.[37] These aeGBR generators have been shown to be less active in schizophrenia patients.[40] Because gamma-band oscillations are assumed to be important for the functional coupling of brain regions[4] even over long distances,[79] the network showing reduced activity in HRP subjects in the present study could be considered as coupled by means of gamma synchronisation as the aeGBR is phase locked to the stimulus. Deficits of the ACC and the DLPFC have consistently been reported in schizophrenia.[52,80–83] Both regions are known to be involved in processing of higher order cognitive processes.[84,85] Accordingly, our data suggest a disturbed gamma-mediated functional interaction between higher order frontal brain regions and auditory cortices during attention demanding auditory information processing in HRP individuals. Because the aeGBR has been described earlier to be generated in the auditory cortex[32,86] as a result of thalamo-cortical interactions,[87] our finding of an aeGBR-specific thalamus activation (in line with a previous observation[46]) could be interpreted as a strong functional coupling of the network via thalamus, which is disturbed in the high-risk state of psychosis. In fact, the thalamus is generally known to play a crucial role for the generation of cortical brain rhythms.[88,89] Stimulation of thalamic nuclei in animals was associated with evoked gamma-band oscillations in the auditory cortex.[90]

The E-HRP and the L-HRP defined in accordance with GNRS criteria[48] have been shown to be characterized by different neurophysiological,[91] neurocognitive,[92] and neuroanatomical[93] changes and it has been suggested that changes encountered in the early high-risk state represent a stable trait indicating increased susceptibility for psychosis, whereas those encountered in the L-HRP might be more closely associated with the impending emergence of psychotic symptoms.[91,93] Thus, the inclusion of subjects of both high-risk states may delimitate the significance of our results. However, in the present study the majority of participants met criteria for the L-HRP and repeating our analysis for the L-HRP fraction of the HRP group did not substantially change our results.

Other limitations, inherent in high-risk studies, consist in the influence of local recruitment criteria (eg, the time of inclusion[94]), in the conversion rates[63] and in the high comorbidity rates, especially for mood, anxiety, substance use and Axis II disorders. These limitations are

usually encountered in high-risk samples[95] and reflected in the present high-risk sample as well. In the present study, there were no significant correlations of neurophysiological findings with the depression (depression/anxiety) factor of the SOPS. Moreover, repeating our analysis for the fraction of HRP subjects without substance related disorders did not substantially change our results. However, in order to conclusively exclude the possibility that our findings reflected unspecific symptoms rather than increased susceptibility to psychosis, a direct comparison depending on transition status at follow-up (ie,emergence or not of a psychotic disorder) would be necessary, which, unfortunately, was not possible in the present sample because of a lack of adequate follow-up information. However, the replicated findings of alterations of the aeGBR across all stages of schizophrenia support our assumption to have investigated a biological marker related to schizophrenia in the present study.

In conclusion, our EEG-informed fMRI approach revealed a disturbed aeGBR-specific network involving thalamus, auditory cortices, and frontal regions such as the ACC and the DLPFC in individuals at clinical high risk for psychosis during performance of a cognitively demanding auditory task. The high-risk state for psychosis reflects the clinical risk for conversion to psychotic disorders including schizophrenia and the aeGBR has repeatedly been shown to be altered in patients with schizophrenia. Therefore the results of our study point towards a potential applicability of aeGBR disturbances as a marker for the prediction of transition of HRP subjects to schizophrenia.

Supplementary Material

Supplementary material is available at http://schizophreniabulletin.oxfordjournals.org.

Funding

German Research Foundation (DFG SFB 936-C6 to C.M.).

Acknowledgments

Parts of this work were prepared in the context of Sebastian Vauth's dissertation at the Faculty of Medicine, University of Hamburg, Hamburg. The authors have declared that there are no conflicts of interest in relation to the subject of this study.

References

1. Başar E. A review of gamma oscillations in healthy subjects and in cognitive impairment. *Int J Psychophysiol*. 2013;90:99–117.
2. Canolty RT, Edwards E, Dalal SS, et al. High gamma power is phase-locked to theta oscillations in human neocortex. *Science*. 2006;313:1626–1628.
3. Fries P, Nikolić D, Singer W. The gamma cycle. *Trends Neurosci*. 2007;30:309–316.
4. Singer W. Neuronal synchrony: a versatile code for the definition of relations? *Neuron*. 1999;24:49–65.
5. Engel AK, Fries P, Singer W. Dynamic predictions: oscillations and synchrony in top-down processing. *Nat Rev Neurosci*. 2001;2:704–716.
6. Uhlhaas PJ, Singer W. Abnormal neural oscillations and synchrony in schizophrenia. *Nat Rev Neurosci*. 2010;11:100–113.
7. Friston KJ. Schizophrenia and the disconnection hypothesis. *Acta Psychiatr Scand Suppl*. 1999;395:68–79.
8. Phillips WA, Silverstein SM. Convergence of biological and psychological perspectives on cognitive coordination in schizophrenia. *Behav Brain Sci*. 2003;26:65–82; discussion 82.
9. van den Heuvel MP, Fornito A. Brain networks in schizophrenia. *Neuropsychol Rev*. 2014;24:32–48.
10. Uhlhaas PJ. Dysconnectivity, large-scale networks and neuronal dynamics in schizophrenia. *Curr Opin Neurobiol*. 2013;23:283–290.
11. Bartos M, Vida I, Jonas P. Synaptic mechanisms of synchronized gamma oscillations in inhibitory interneuron networks. *Nat Rev Neurosci*. 2007;8:45–56.
12. Sohal VS, Zhang F, Yizhar O, Deisseroth K. Parvalbumin neurons and gamma rhythms enhance cortical circuit performance. *Nature*. 2009;459:698–702.
13. Gandal MJ, Edgar JC, Klook K, Siegel SJ. Gamma synchrony: towards a translational biomarker for the treatment-resistant symptoms of schizophrenia. *Neuropharmacology*. 2012;62:1504–1518.
14. Uhlhaas PJ, Singer W. High-frequency oscillations and the neurobiology of schizophrenia. *Dialogues Clin Neurosci*. 2013;15:301–13.
15. Lisman JE, Coyle JT, Green RW, et al. Circuit-based framework for understanding neurotransmitter and risk gene interactions in schizophrenia. *Trends Neurosci*. 2008;31:234–242.
16. Krishnan GP, Vohs JL, Hetrick WP, et al. Steady state visual evoked potential abnormalities in schizophrenia. *Clin Neurophysiol*. 2005;116:614–624.
17. Spencer KM, Nestor PG, Niznikiewicz MA, Salisbury DF, Shenton ME, McCarley RW. Abnormal neural synchrony in schizophrenia. *J Neurosci*. 2003;23:7407–7411.
18. Spencer KM, Nestor PG, Perlmutter R, et al. Neural synchrony indexes disordered perception and cognition in schizophrenia. *Proc Natl Acad Sci U S A*. 2004;101:17288–17293.
19. Kwon JS, O'Donnell BF, Wallenstein GV, et al. Gamma frequency-range abnormalities to auditory stimulation in schizophrenia. *Arch Gen Psychiatry*. 1999;56:1001–1005.
20. Spencer KM, Salisbury DF, Shenton ME, McCarley RW. Gamma-band auditory steady-state responses are impaired in first episode psychosis. *Biol Psychiatry*. 2008;64:369–375.
21. Vierling-Claassen D, Siekmeier P, Stufflebeam S, Kopell N. Modeling GABA alterations in schizophrenia: a link between impaired inhibition and altered gamma and beta range auditory entrainment. *J Neurophysiol*. 2008;99:2656–2671.
22. Wilson TW, Hernandez OO, Asherin RM, Teale PD, Reite ML, Rojas DC. Cortical gamma generators suggest abnormal auditory circuitry in early-onset psychosis. *Cereb Cortex*. 2008;18:371–378.
23. Teale P, Collins D, Maharajh K, Rojas DC, Kronberg E, Reite M. Cortical source estimates of gamma band amplitude and phase are different in schizophrenia. *Neuroimage*. 2008;42:1481–1489.

24. Light GA, Hsu JL, Hsieh MH, et al. Gamma band oscillations reveal neural network cortical coherence dysfunction in schizophrenia patients. *Biol Psychiatry*. 2006;60:1231–1240.
25. Spencer KM, Niznikiewicz MA, Shenton ME, McCarley RW. Sensory-evoked gamma oscillations in chronic schizophrenia. *Biol Psychiatry*. 2008;63:744–747.
26. Gallinat J, Winterer G, Herrmann CS, Senkowski D. Reduced oscillatory gamma-band responses in unmedicated schizophrenic patients indicate impaired frontal network processing. *Clin Neurophysiol*. 2004;115:1863–1874.
27. Haig AR, Gordon E, De Pascalis V, Meares RA, Bahramali H, Harris A. Gamma activity in schizophrenia: evidence of impaired network binding? *Clin Neurophysiol*. 2000;111:1461–1468.
28. Lee KH, Williams LM, Haig A, Goldberg E, Gordon E. An integration of 40 Hz Gamma and phasic arousal: novelty and routinization processing in schizophrenia. *Clin Neurophysiol*. 2001;112:1499–1507.
29. Roach BJ, Mathalon DH. Event-related EEG time-frequency analysis: an overview of measures and an analysis of early gamma band phase locking in schizophrenia. *Schizophr Bull*. 2008;34:907–926.
30. Symond MP, Harris AW, Gordon E, Williams LM. "Gamma synchrony" in first-episode schizophrenia: a disorder of temporal connectivity? *Am J Psychiatry* 2005;162:459–65.
31. Cho RY, Konecky RO, Carter CS. Impairments in frontal cortical gamma synchrony and cognitive control in schizophrenia. *Proc Natl Acad Sci U S A*. 2006;103:19878–19883.
32. Pantev C, Makeig S, Hoke M, Galambos R, Hampson S, Gallen C. Human auditory evoked gamma-band magnetic fields. *Proc Natl Acad Sci U S A*. 1991;88:8996–9000.
33. Tiitinen H, Sinkkonen J, Reinikainen K, Alho K, Lavikainen J, Näätänen R. Selective attention enhances the auditory 40-Hz transient response in humans. *Nature*. 1993;364:59–60.
34. Tiitinen H, May P, Näätänen R. The transient 40-Hz response, mismatch negativity, and attentional processes in humans. *Prog Neuropsychopharmacol Biol Psychiatry*. 1997;21:751–771.
35. Gurtubay IG, Alegre M, Labarga A, Malanda A, Artieda J. Gamma band responses to target and non-target auditory stimuli in humans. *Neurosci Lett*. 2004;367:6–9.
36. Herrmann CS, Fründ I, Lenz D. Human gamma-band activity: a review on cognitive and behavioral correlates and network models. *Neurosci Biobehav Rev*. 2010;34:981–992.
37. Mulert C, Leicht G, Pogarell O, et al. Auditory cortex and anterior cingulate cortex sources of the early evoked gamma-band response: relationship to task difficulty and mental effort. *Neuropsychologia*. 2007;45:2294–2306.
38. Leicht G, Andreou C, Polomac N, et al. Reduced auditory evoked gamma band response and cognitive processing deficits in first episode schizophrenia [published online ahead of print March, 2015]. *World J Biol Psychiatry*. doi:10.3109/15622975.2015.1017605
39. Taylor GW, McCarley RW, Salisbury DF. Early auditory gamma band response abnormalities in first hospitalized schizophrenia. *Suppl Clin Neurophysiol*. 2013;62:131–145.
40. Leicht G, Kirsch V, Giegling I, et al. Reduced early auditory evoked gamma-band response in patients with schizophrenia. *Biol Psychiatry*. 2010;67:224–231.
41. Leicht G, Karch S, Karamatskos E, et al. Alterations of the early auditory evoked gamma-band response in first-degree relatives of patients with schizophrenia: hints to a new intermediate phenotype. *J Psychiatr Res*. 2011;45:699–705.
42. Hall MH, Taylor G, Salisbury DF, Levy DL. Sensory gating event-related potentials and oscillations in schizophrenia patients and their unaffected relatives. *Schizophr Bull*. 2011;37:1187–1199.
43. Tsuang MT, Faraone SV, Lyons MJ. Identification of the phenotype in psychiatric genetics. *Eur Arch Psychiatry Clin Neurosci*. 1993;243:131–142.
44. Hall MH, Taylor G, Sham P, et al. The early auditory gamma-band response is heritable and a putative endophenotype of schizophrenia. *Schizophr Bull*. 2011;37:778–787.
45. Perez VB, Roach BJ, Woods SW, et al. Early auditory gamma-band responses in patients at clinical high risk for schizophrenia. *Suppl Clin Neurophysiol*. 2013;62:147–162.
46. Mulert C, Leicht G, Hepp P, et al. Single-trial coupling of the gamma-band response and the corresponding BOLD signal. *Neuroimage*. 2010;49:2238–2247.
47. Wolwer W, Baumann A, Bechdolf A, et al. The German Research Network on Schizophrenia--impact on the management of schizophrenia. *Dialogues Clin Neurosci*. 2006;8:115–121.
48. Ruhrmann S, Schultze-Lutter F, Klosterkötter J. Early detection and intervention in the initial prodromal phase of schizophrenia. *Pharmacopsychiatry*. 2003;36(suppl 3):S162–S167.
49. Sheehan DV, Lecrubier Y, Sheehan KH, et al. The Mini-International Neuropsychiatric Interview (M.I.N.I.): the development and validation of a structured diagnostic psychiatric interview for DSM-IV and ICD-10. *J Clin Psychiatry*. 1998;59(Suppl 20):22–33; quiz 4–57.
50. Miller TJ, McGlashan TH, Rosen JL, et al. Prodromal assessment with the structured interview for prodromal syndromes and the scale of prodromal symptoms: predictive validity, interrater reliability, and training to reliability. *Schizophr Bull*. 2003;29:703–715.
51. Hawkins KA, McGlashan TH, Quinlan D, et al. Factorial structure of the Scale of Prodromal Symptoms. *Schizophr Res*. 2004;68:339–347.
52. Mulert C, Gallinat J, Pascual-Marqui R, et al. Reduced event-related current density in the anterior cingulate cortex in schizophrenia. *Neuroimage*. 2001;13:589–600.
53. Hall DA, Haggard MP, Akeroyd MA, et al. "Sparse" temporal sampling in auditory fMRI. *Hum Brain Mapp*. 1999;7:213–223.
54. Mulert C, Jäger L, Schmitt R, et al. Integration of fMRI and simultaneous EEG: towards a comprehensive understanding of localization and time-course of brain activity in target detection. *Neuroimage*. 2004;22:83–94.
55. Mulert C, Seifert C, Leicht G, et al. Single-trial coupling of EEG and fMRI reveals the involvement of early anterior cingulate cortex activation in effortful decision making. *Neuroimage*. 2008;42:158–168.
56. Allen PJ, Polizzi G, Krakow K, Fish DR, Lemieux L. Identification of EEG events in the MR scanner: the problem of pulse artifact and a method for its subtraction. *Neuroimage*. 1998;8:229–239.
57. Eichele T, Specht K, Moosmann M, et al. Assessing the spatiotemporal evolution of neuronal activation with single-trial event-related potentials and functional MRI. *Proc Natl Acad Sci U S A*. 2005;102:17798–17803.
58. Karch S, Voelker JM, Thalmeier T, et al. Deficits during Voluntary Selection in Adult Patients with ADHD: New Insights from Single-Trial Coupling of Simultaneous EEG/fMRI. *Front Psychiatry*. 2014;5:41.
59. Karch S, Feuerecker R, Leicht G, et al. Separating distinct aspects of the voluntary selection between response alternatives: N2- and P3-related BOLD responses. *Neuroimage*. 2010;51:356–364.

60. Jaspers-Fayer F, Ertl M, Leicht G, Leupelt A, Mulert C. Single-trial EEG-fMRI coupling of the emotional auditory early posterior negativity. *Neuroimage*. 2012;62:1807–1814.
61. Polomac N, Leicht G, Nolte G, et al. Generators and connectivity of the early auditory evoked gamma band response. *Brain Topogr*. 2015.
62. Tallon-Baudry C, Bertrand O, Hénaff MA, Isnard J, Fischer C. Attention modulates gamma-band oscillations differently in the human lateral occipital cortex and fusiform gyrus. *Cereb Cortex*. 2005;15:654–662.
63. Fusar-Poli P, Bonoldi I, Yung AR, et al. Predicting psychosis: meta-analysis of transition outcomes in individuals at high clinical risk. *Arch Gen Psychiatry*. 2012;69:220–229.
64. Gottesman II, Gould TD. The endophenotype concept in psychiatry: etymology and strategic intentions. *Am J Psychiatry*. 2003;160:636–645.
65. Benes FM. Neural circuitry models of schizophrenia: is it dopamine, GABA, glutamate, or something else? *Biol Psychiatry*. 2009;65:1003–1005.
66. Benes FM, Lim B, Matzilevich D, Walsh JP, Subburaju S, Minns M. Regulation of the GABA cell phenotype in hippocampus of schizophrenics and bipolars. *Proc Natl Acad Sci U S A*. 2007;104:10164–10169.
67. Zhang ZJ, Reynolds GP. A selective decrease in the relative density of parvalbumin-immunoreactive neurons in the hippocampus in schizophrenia. *Schizophr Res*. 2002;55:1–10.
68. Kalus P, Senitz D, Beckmann H. Altered distribution of parvalbumin-immunoreactive local circuit neurons in the anterior cingulate cortex of schizophrenic patients. *Psychiatry Res*. 1997;75:49–59.
69. Woo TU, Walsh JP, Benes FM. Density of glutamic acid decarboxylase 67 messenger RNA-containing neurons that express the N-methyl-D-aspartate receptor subunit NR2A in the anterior cingulate cortex in schizophrenia and bipolar disorder. *Arch Gen Psychiatry*. 2004;61:649–657.
70. Lodge DJ, Behrens MM, Grace AA. A loss of parvalbumin-containing interneurons is associated with diminished oscillatory activity in an animal model of schizophrenia. *J Neurosci*. 2009;29:2344–2354.
71. Lewis DA, Moghaddam B. Cognitive dysfunction in schizophrenia: convergence of gamma-aminobutyric acid and glutamate alterations. *Arch Neurol*. 2006;63:1372–1376.
72. Hashimoto T, Arion D, Unger T, et al. Alterations in GABA-related transcriptome in the dorsolateral prefrontal cortex of subjects with schizophrenia. *Mol Psychiatry*. 2008;13:147–161.
73. Mulert C. Simultaneous EEG and fMRI: towards the characterization of structure and dynamics of brain networks. *Dialogues in clinical neuroscience* 2013;15:381–6.
74. Mukamel R, Gelbard H, Arieli A, Hasson U, Fried I, Malach R. Coupling between neuronal firing, field potentials, and FMRI in human auditory cortex. *Science*. 2005;309:951–954.
75. Niessing J, Ebisch B, Schmidt KE, Niessing M, Singer W, Galuske RA. Hemodynamic signals correlate tightly with synchronized gamma oscillations. *Science*. 2005;309:948–951.
76. Logothetis NK. The neural basis of the blood-oxygen-level-dependent functional magnetic resonance imaging signal. *Philos Trans R Soc Lond B Biol Sci*. 2002;357:1003–1037.
77. Logothetis NK, Pauls J, Augath M, Trinath T, Oeltermann A. Neurophysiological investigation of the basis of the fMRI signal. *Nature*. 2001;412:150–157.
78. Kilner JM, Mattout J, Henson R, Friston KJ. Hemodynamic correlates of EEG: a heuristic. *Neuroimage*. 2005;28:280–286.
79. Rodriguez E, George N, Lachaux JP, Martinerie J, Renault B, Varela FJ. Perception's shadow: long-distance synchronization of human brain activity. *Nature*. 1999;397:430–433.
80. Walton E, Geisler D, Lee PH, et al. Prefrontal inefficiency is associated with polygenic risk for schizophrenia. *Schizophr Bull*. 2014;40:1263–1271.
81. Dehaene S, Artiges E, Naccache L, et al. Conscious and subliminal conflicts in normal subjects and patients with schizophrenia: the role of the anterior cingulate. *Proc Natl Acad Sci U S A*. 2003;100:13722–13727.
82. Bersani FS, Minichino A, Fojanesi M, et al. Cingulate Cortex in Schizophrenia: its relation with negative symptoms and psychotic onset. A review study. *Eur Rev Med Pharmacol Sci*. 2014;18:3354–3367.
83. Goldstein JM, Goodman JM, Seidman LJ, et al. Cortical abnormalities in schizophrenia identified by structural magnetic resonance imaging. *Arch Gen Psychiatry*. 1999;56:537–547.
84. Wesley MJ, Bickel WK. Remember the future II: meta-analyses and functional overlap of working memory and delay discounting. *Biol Psychiatry*. 2014;75:435–448.
85. Botvinick MM, Cohen JD, Carter CS. Conflict monitoring and anterior cingulate cortex: an update. *Trends Cogn Sci*. 2004;8:539–546.
86. Schadow J, Lenz D, Dettler N, Fründ I, Herrmann CS. Early gamma-band responses reflect anticipatory top-down modulation in the auditory cortex. *Neuroimage*. 2009;47:651–658.
87. Ribary U, Ioannides AA, Singh KD, et al. Magnetic field tomography of coherent thalamocortical 40-Hz oscillations in humans. *Proc Natl Acad Sci U S A*. 1991;88:11037–11041.
88. Steriade M. Grouping of brain rhythms in corticothalamic systems. *Neuroscience*. 2006;137:1087–1106.
89. Lopes da Silva F. Neural mechanisms underlying brain waves: from neural membranes to networks. *Electroencephalogr Clin Neurophysiol*. 1991;79:81–93.
90. Sukov W, Barth DS. Cellular mechanisms of thalamically evoked gamma oscillations in auditory cortex. *J Neurophysiol*. 2001;85:1235–1245.
91. Frommann I, Brinkmeyer J, Ruhrmann S, et al. Auditory P300 in individuals clinically at risk for psychosis. *Int J Psychophysiol*. 2008;70:192–205.
92. Frommann I, Pukrop R, Brinkmeyer J, et al. Neuropsychological profiles in different at-risk states of psychosis: executive control impairment in the early–and additional memory dysfunction in the late–prodromal state. *Schizophr Bull*. 2011;37:861–873.
93. Koutsouleris N, Schmitt GJ, Gaser C, et al. Neuroanatomical correlates of different vulnerability states for psychosis and their clinical outcomes. *Br J Psychiatry*. 2009;195:218–226.
94. Nelson B, Yuen HP, Wood SJ, et al. Long-term follow-up of a group at ultra high risk ("prodromal") for psychosis: the PACE 400 study. *JAMA Psychiatry*. 2013;70:793–802.
95. Fusar-Poli P, Borgwardt S, Bechdolf A, et al. The psychosis high-risk state: a comprehensive state-of-the-art review. *JAMA Psychiatry*. 2013;70:107–120.